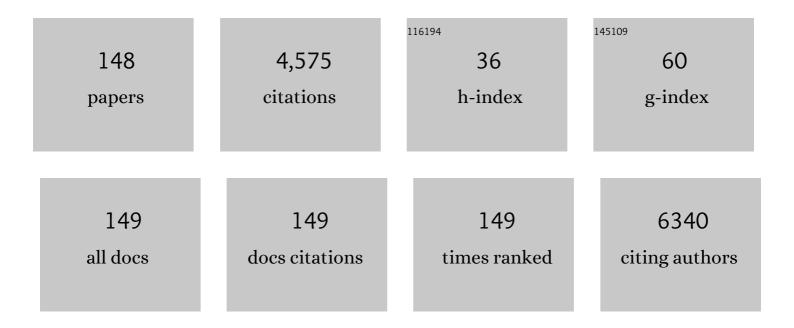
## S Ponnusamy

List of Publications by Year in descending order

Source: https://exaly.com/author-pdf/4304987/publications.pdf Version: 2024-02-01



#	Article	IF	CITATIONS
1	Effect of Sr doping in ZnO microspheres for solar light-driven photodegradation of organic pollutants. Journal of Materials Science: Materials in Electronics, 2022, 33, 8777-8788.	1.1	6
2	Synergic effect of Sn-doped TiO2 nanostructures for enhanced visible light photocatalysis. Journal of Materials Science: Materials in Electronics, 2022, 33, 9066-9084.	1.1	5
3	Efficient catalytic activity of BiVO4 nanostructures by crystal facet regulation for environmental remediation. Chemosphere, 2022, 289, 133097.	4.2	22
4	High-performance carbon derived from chickpea skin via microwave and slow pyrolysis for supercapacitors. Materials Letters, 2022, 314, 131872.	1.3	3
5	Controlled grain boundary interfaces of reduced graphene oxide in Ag2Se matrix for low lattice thermal conductivity and enhanced power factor for thermoelectric applications. Journal of Power Sources, 2022, 525, 231045.	4.0	10
6	A facile synthesis of Zn-doped TiO2 nanostructures for enhanced photocatalytic performance. Journal of Materials Science: Materials in Electronics, 2022, 33, 9798-9813.	1.1	2
7	Improved supercapacitor performance based on sustainable synthesis using chemically activated porous carbon. Journal of Alloys and Compounds, 2022, 906, 164287.	2.8	12
8	Conductometric NO2 gas sensor based on Co-incorporated MoS2 nanosheets for room temperature applications. Sensors and Actuators B: Chemical, 2022, 360, 131600.	4.0	38
9	Interface driven energy-filtering and phonon scattering of polyaniline incorporated ultrathin layered molybdenum disulphide nanosheets for promising thermoelectric performance. Journal of Colloid and Interface Science, 2021, 584, 295-309.	5.0	20
10	High-performance electrocatalytic and cationic substitution in Cu2ZnSnS4 as a low-cost counter electrode for Pt-free dye-sensitized solar cells. Journal of Materials Science, 2021, 56, 4135-4150.	1.7	13
11	Surface Modification of ZnO Nanowires with CuO: A Tool to Realize Highly-Sensitive H2S Sensor. Physics of the Solid State, 2021, 63, 460-467.	0.2	3
12	A novel strategy of nanosized herbal Plectranthus amboinicus, Phyllanthus niruri and Euphorbia hirta treated TiO2 nanoparticles for antibacterial and anticancer activities. Bioprocess and Biosystems Engineering, 2021, 44, 1593-1616.	1.7	9
13	NO2 sensor based on Al modified ZnO nanowires. Materials Science in Semiconductor Processing, 2021, 134, 106027.	1.9	14
14	Oxide-based catalysis: tailoring surface structures via organic ligands and related interfacial charge carrier for environmental remediation. RSC Advances, 2021, 11, 19059-19069.	1.7	0
15	Interface enriched highly interlaced layered MoS <sub>2</sub> /NiS <sub>2</sub> nanocomposites for the photocatalytic degradation of rhodamine B dye. RSC Advances, 2021, 11, 19283-19293.	1.7	17
16	Hydrothermal synthesis of pure and bio modified TiO2: Characterization, evaluation of antibacterial activity against gram positive and gram negative bacteria and anticancer activity against KB Oral cancer cell line. Arabian Journal of Chemistry, 2020, 13, 3484-3497.	2.3	34
17	Syntheses and characterization of Syzygium aromaticum, Elettaria cardamomum and Cinnamomum verum modified TiO2 and their biological applications. Materials Science in Semiconductor Processing, 2020, 105, 104724.	1.9	8
18	Growth and influence of Gd doping on ZnO nanostructures for enhanced optical, structural properties and gas sensing applications. Applied Surface Science, 2020, 499, 143857.	3.1	60

#	Article	IF	CITATIONS
19	Effect of ethylenediamine on morphology of 2D Co-Mo-S@NG hybrids and their enhanced electrocatalytic activity for DSSCs application. Materials Science in Semiconductor Processing, 2020, 105, 104725.	1.9	7
20	Hierarchical NiO@NiS@graphene nanocomposite as a sustainable counter electrode for Pt free dye-sensitized solar cell. Applied Surface Science, 2020, 501, 144010.	3.1	44
21	Synthesis and functional properties of nanostructured Gd-doped WO3/TiO2 composites for sensing applications. Materials Science in Semiconductor Processing, 2020, 105, 104732.	1.9	28
22	Synthesis and characterization of TiO2 nanorods by hydrothermal method with different pH conditions and their photocatalytic activity. Applied Surface Science, 2020, 500, 144058.	3.1	75
23	Thermoelectric performance of Cu-doped MoS2 layered nanosheets for low grade waste heat recovery. Applied Surface Science, 2020, 505, 144066.	3.1	30
24	Cytotoxicity assessment of chitosan coated CdS nanoparticles for bio-imaging applications. Applied Surface Science, 2020, 499, 143817.	3.1	44
25	One-step fabrication of ultrathin layered 1T@2H phase MoS2 with high catalytic activity based counter electrode for photovoltaic devices. Journal of Materials Science and Technology, 2020, 51, 94-101.	5.6	30
26	Bio-modified TiO2 nanoparticles with Withania somnifera, Eclipta prostrata and Glycyrrhiza glabra for anticancer and antibacterial applications. Materials Science and Engineering C, 2020, 108, 110457.	3.8	40
27	Improvement of Photocatalytic Activity by Zn Doping in Cu2O. Physics of the Solid State, 2020, 62, 1796-1802.	0.2	9
28	Effect of densification technique and carrier concentration on the thermoelectric properties of n-type Cu1.45Ni1.45Te2 ternary compound. CrystEngComm, 2020, 22, 8100-8109.	1.3	2
29	Enhanced seebeck coefficient and low thermal conductivity of Cu2SexTe1-x solid solutions via minority carrier blocking and interfacial effects. Journal of Alloys and Compounds, 2020, 835, 155188.	2.8	9
30	Hydrothermal syntheses and characterization of bio-modified TiO2 nanoparticles with Aqua Rosa and Protein powder for their biological applications. Applied Surface Science, 2019, 494, 989-999.	3.1	6
31	Hydrothermal synthesis of C doped ZnO nanoparticles coupled with BiVO4 and their photocatalytic performance under the visible light irradiation. Applied Surface Science, 2019, 494, 771-782.	3.1	29
32	Effect of organic ligand on ZnO nanostructures and to investigate the photocatalytic activity under visible light illumination. Materials Science in Semiconductor Processing, 2019, 103, 104608.	1.9	5
33	Synthesis and photocatalytic activity of Gd doped ZnO nanoparticles for enhanced degradation of methylene blue under visible light. Materials Science in Semiconductor Processing, 2019, 103, 104622.	1.9	81
34	Design and fabrication of PANI/GO nanocomposite for enhanced room-temperature thermoelectric application. Applied Surface Science, 2019, 493, 1350-1360.	3.1	44
35	Synergistic effect and enhanced electrical properties of TiO2/SnO2/ZnO nanostructures as electron extraction layer for solar cell application. Applied Surface Science, 2019, 498, 143702.	3.1	22
36	Growth of Fe doped ZnO nanoellipsoids for selective NO2 gas sensing application. Chemical Physics Letters, 2019, 734, 136725.	1.2	29

#	Article	IF	CITATIONS
37	Hierarchically porous structured carbon derived from peanut shell as an enhanced high rate anode for lithium ion batteries. Applied Surface Science, 2019, 492, 464-472.	3.1	35
38	Etching and microhardness studies of pure and doped nonlinear optical crystals of Hippuric acid. Applied Surface Science, 2019, 491, 123-127.	3.1	0
39	Zn and Sr co-doped TiO2 mesoporous nanospheres as photoanodes in dye sensitized solar cell. Materials Chemistry and Physics, 2019, 234, 259-267.	2.0	13
40	Ultra-low thermal conductivity via interfacial phonon scattering in PbTe hoppercubes/PbTeO3 microrods for thermoelectric applications. Journal of Alloys and Compounds, 2019, 799, 26-35.	2.8	3
41	Highly efficient 3-D hierarchical Bi2WO6 catalyst for environmental remediation. Applied Surface Science, 2019, 488, 696-706.	3.1	29
42	Enhanced charge transfer and separation of hierarchical CuO/ZnO composites: The synergistic effect of photocatalysis for the mineralization of organic pollutant in water. Applied Surface Science, 2019, 484, 884-891.	3.1	85
43	Metal sulfide nanosheet–nitrogen-doped graphene hybrids as low-cost counter electrodes for dye-sensitized solar cells. Applied Surface Science, 2019, 480, 177-185.	3.1	18
44	Surfactant free controllable synthesis of 2D – 1D ZnO hierarchical nanostructure and its gas sensing properties. Applied Surface Science, 2018, 449, 838-845.	3.1	22
45	Electrochemical Behavior of Biomedical Titanium Alloys Coated with Diamond Carbon in Hanks' Solution. Journal of Materials Engineering and Performance, 2018, 27, 1635-1641.	1.2	16
46	Enhanced photon collection of high surface area carbonate-doped mesoporous TiO2 nanospheres in dye sensitized solar cells. Materials Research Bulletin, 2018, 101, 353-362.	2.7	32
47	Spectral, optical, etching, second harmonic generation (SHG) and laser damage threshold studies of nonlinear optical crystals of I-Histidine bromide. Applied Surface Science, 2018, 449, 92-95.	3.1	10
48	ZnO hierarchical 3D-flower like architectures and their gas sensing properties at room temperature. Applied Surface Science, 2018, 449, 314-321.	3.1	32
49	Effect of Al doping on the electrical and optical properties of TiO2 embedded Graphene Oxide nanosheets for opto-electronic applications. Applied Surface Science, 2018, 449, 332-339.	3.1	13
50	Ultra-fast photocatalytic and dye-sensitized solar cell performances of mesoporous TiO2 nanospheres. Applied Surface Science, 2018, 449, 729-735.	3.1	16
51	Chemical synthesis of highly size-confined triethylamine-capped \$\$hbox {TiO}_{2}\$\$ TiO 2 nanoparticles and its dye-sensitized solar cell performance. Bulletin of Materials Science, 2018, 41, 1.	0.8	1
52	Tuning the selectivity of NH3 gas sensing response using Cu-doped ZnO nanostructures. Sensors and Actuators A: Physical, 2018, 269, 331-341.	2.0	93
53	Sensitivity enhancement of ammonia gas sensor based on Ag/ZnO flower and nanoellipsoids at low temperature. Sensors and Actuators B: Chemical, 2018, 255, 672-683.	4.0	199
54	Biocompatible response of hydroxyapatite coated on near-β titanium alloys by E-beam evaporation method. Biocatalysis and Agricultural Biotechnology, 2018, 15, 364-369.	1.5	14

#	Article	IF	CITATIONS
55	Ultrathin layered MoS <sub>2</sub> nanosheets with rich active sites for enhanced visible light photocatalytic activity. RSC Advances, 2018, 8, 26664-26675.	1.7	54
56	Synthesis of ZnO/SrO nanocomposites for enhanced photocatalytic activity under visible light irradiation. Applied Surface Science, 2017, 418, 147-155.	3.1	36
57	Fabrication of the flexible nanogenerator from BTO nanopowders on graphene coated PMMA substrates by sol-gel method. Materials Chemistry and Physics, 2017, 192, 274-281.	2.0	24
58	Surfactant free synthesis of CdS nanospheres, microstructural analysis, chemical bonding, optical properties and photocatalytic activities. Superlattices and Microstructures, 2017, 104, 247-257.	1.4	36
59	Functional properties and enhanced visible light photocatalytic performance of V3O4 nanostructures decorated ZnO nanorods. Applied Surface Science, 2017, 418, 171-178.	3.1	19
60	Crystal growth and properties of novel organic nonlinear optical crystals of 4-Nitrophenol urea. Materials Chemistry and Physics, 2017, 195, 224-228.	2.0	10
61	Visible light induced photocatalytic degradation of methylene blue and rhodamine B from the catalyst of CdS nanowire. Chemical Physics Letters, 2017, 684, 126-134.	1.2	47
62	Synthesis of cluster like TiO2 mesoporous spheres and nanorods and their applications in dye-sensitized solar cells. Journal of Materials Science: Materials in Electronics, 2017, 28, 14935-14943.	1.1	0
63	Growth, microstructure, structural and optical properties of PVP-capped CdS nanoflowers for efficient photocatalytic activity of Rhodamine B. Materials Research Bulletin, 2017, 94, 190-198.	2.7	37
64	Low temperature ammonia gas sensor based on Mn-doped ZnO nanoparticle decorated microspheres. Journal of Alloys and Compounds, 2017, 721, 182-190.	2.8	122
65	Enhancement of power factor by energy filtering effect in hierarchical BiSbTe3 nanostructures for thermoelectric applications. Applied Surface Science, 2017, 418, 246-251.	3.1	17
66	Hydrothermal growth of highly monodispersed TiO2 nanoparticles: Functional properties and dye-sensitized solar cell performance. Applied Surface Science, 2017, 418, 186-193.	3.1	7
67	0.8 V nanogenerator for mechanical energy harvesting using bismuth titanate–PDMS nanocomposite. Applied Surface Science, 2017, 418, 362-368.	3.1	21
68	Influence of organic ligands on the formation and functional properties of CdS nanostructures. Applied Surface Science, 2017, 418, 346-351.	3.1	9
69	Controlled structural and compositional characteristic of visible light active ZnO/CuO photocatalyst for the degradation of organic pollutant. Applied Surface Science, 2017, 418, 103-112.	3.1	137
70	Influence of Al doping on the structural, morphological, optical, and gas sensing properties of ZnO nanorods. Journal of Alloys and Compounds, 2017, 698, 555-564.	2.8	162
71	Microstructure, structural, optical and piezoelectric properties of BiFeO3 nanopowder synthesized from sol-gel. Current Applied Physics, 2017, 17, 409-416.	1.1	26
72	Controlled synthesis of Ni-doped ZnO hexagonal microdiscs and their gas sensing properties at low temperature. Chemical Physics Letters, 2017, 689, 92-99.	1.2	56

#	Article	IF	CITATIONS
73	Synergetic effect of CuS@ZnS nanostructures on photocatalytic degradation of organic pollutant under visible light irradiation. RSC Advances, 2017, 7, 34366-34375.	1.7	40
74	Highly efficient dye-sensitized solar cell performance from template derived high surface area mesoporous TiO <sub>2</sub> nanospheres. RSC Advances, 2016, 6, 68092-68099.	1.7	20
75	Photocatalytic properties of Mn-doped NiO spherical nanoparticles synthesized from sol-gel method. Optik, 2016, 127, 10727-10734.	1.4	93
76	Enhanced visible light induced photocatalytic activity on the degradation of organic pollutants by SnO nanoparticle decorated hierarchical ZnO nanostructures. RSC Advances, 2016, 6, 89721-89731.	1.7	42
77	ZnS/CuS nanocomposites: an effective strategy to transform UV active ZnS to UV and Vis light active ZnS. Journal of Materials Science: Materials in Electronics, 2016, 27, 9022-9033.	1.1	8
78	Effect of organic-ligands on the toxicity profiles of CdS nanoparticles and functional properties. Colloids and Surfaces B: Biointerfaces, 2015, 126, 407-413.	2.5	17
79	Effect of TEA on the structural and magnetic properties of ferromagnetic ZnFe2O4 nanoparticles. Journal of Materials Science: Materials in Electronics, 2015, 26, 547-553.	1.1	4
80	Solvothermal growth of diethylamine capped TiO2 nanoparticles and functional properties. Journal of Materials Science: Materials in Electronics, 2015, 26, 2380-2383.	1.1	1
81	Growth and characterization of a third order nonlinear optical single crystal: Ethylenediamine-4-nitrophenolate monohydrate. Materials Research Bulletin, 2015, 70, 809-816.	2.7	19
82	Chemical synthesis and functional properties of multi-ligands passivated lead sulfide nanoparticles. Materials Letters, 2015, 158, 75-79.	1.3	3
83	Growth and characterization of Piperazinium adipate: A third order NLO single crystal. Journal of Crystal Growth, 2015, 426, 103-109.	0.7	42
84	Fabrication of bistable switching device using CdS nanorods embedded in PMMA (polymethylmethacrylate) nanocomposite. Journal of Materials Science: Materials in Electronics, 2015, 26, 9010-9015.	1.1	6
85	Chemical synthesis and properties of spindle-like CuO nanostructures with porous nature. Materials Letters, 2015, 139, 59-62.	1.3	17
86	Amino acid-mediated synthesis of zinc oxide nanostructures and evaluation of their facet-dependent antimicrobial activity. Colloids and Surfaces B: Biointerfaces, 2014, 117, 233-239.	2.5	67
87	Investigation of photocatalytic behavior of l-aspartic acid stabilized Zn(1â^'x)MnxS solid solutions on methylene blue. Applied Catalysis A: General, 2014, 476, 1-8.	2.2	12
88	Controlled synthesis and morphological investigation of self-assembled CuO nanostructures. Materials Letters, 2014, 121, 129-132.	1.3	20
89	Structural, morphological and magnetic properties of hydrothermally synthesized ZnFe2O4 nanoparticles. Journal of Materials Science: Materials in Electronics, 2014, 25, 2583-2588.	1.1	14
90	One pot facile hydrothermal synthesis of superparamagnetic ZnFe2O4 nanoparticles and their properties. Journal of Sol-Gel Science and Technology, 2014, 71, 147-151.	1.1	13

#	Article	IF	CITATIONS
91	Synthesis of dumbbell shaped ZnO crystals using one-pot hydrothermal method and their characterisations. Materials Letters, 2014, 122, 230-233.	1.3	10
92	Chemical synthesis and functional properties of hexamethylenetetramine capped ZnSe nanorods. Materials Letters, 2014, 125, 32-35.	1.3	4
93	Synthesis and characterization of NiFe2O4 nanoparticles and nanorods. Journal of Alloys and Compounds, 2013, 563, 6-11.	2.8	169
94	Chemical synthesis and functional properties of magnesium doped ZnSe nanoparticles. Materials Letters, 2013, 100, 54-57.	1.3	14
95	Synthesis of superparamagnetic ZnFe2O4 nanoparticle by surfactant assisted hydrothermal method. Journal of Materials Science: Materials in Electronics, 2013, 24, 4279-4283.	1.1	25
96	Synthesis of ZnO nanoflakes by the wet chemical method in the presence of Pb2+ alien cation and their structural and morphological properties. Materials Letters, 2013, 106, 59-62.	1.3	2
97	Synthesis and characterization of SnS/ZnO nanocomposite by chemical method. Journal of Materials Science: Materials in Electronics, 2013, 24, 4807-4811.	1.1	5
98	Synthesis, growth, spectral, thermal, mechanical and optical properties of piperazinium (meso)tartrate crystal: A third order nonlinear optical material. Journal of Crystal Growth, 2013, 363, 211-219.	0.7	69
99	Chemical synthesis and functional properties of monodispersed lanthanum phosphate nanorods. Materials Letters, 2013, 112, 16-19.	1.3	2
100	Growth and characterization of piperazinium 4-nitrophenolate monohydrate (PNP): A third order nonlinear optical material. Optical Materials, 2013, 35, 1327-1334.	1.7	60
101	Preparation of N-methylaniline capped mesoporous TiO2 spheres by simple wet chemical method. Materials Research Bulletin, 2013, 48, 1541-1544.	2.7	2
102	Formation and morphological investigation of petal-like cadmium sulphide nanostructures. Optical Materials, 2013, 35, 1652-1658.	1.7	7
103	Morphology-directed synthesis of ZnO nanostructures and their antibacterial activity. Colloids and Surfaces B: Biointerfaces, 2013, 105, 24-30.	2.5	86
104	Synthesis, Properties and Heating Characteristics of Bovine Serum Albumin Coated Fe <sub>3</sub> O <sub>4</sub> Magnetic Fluid for Magnetic Fluid Hyperthermia Application. Science of Advanced Materials, 2013, 5, 1250-1255.	0.1	2
105	Hydrothermal growth of high surface area anatase TiO2 nanoparticles for dye sensitized solar cell. , 2012, , .		0
106	Formation of anatase TiO2 nanospheres by simple polymer gel technique. , 2012, , .		0
107	Synthesis, studies and growth mechanism of ferromagnetic NiFe2O4 nanosheet. Applied Surface Science, 2012, 258, 6648-6652.	3.1	69
108	Structural, thermal, dielectric and magnetic properties of NiFe2O4 nanoleaf. Journal of Alloys and Compounds, 2012, 537, 203-207.	2.8	29

#	Article	IF	CITATIONS
109	Structural and morphological evolution of CdS nanosheets-based superstructures by surfactant assisted solvothermal method. Materials Chemistry and Physics, 2012, 136, 1038-1043.	2.0	19
110	From zinc oxide nanoparticles to microflowers: A study of growth kinetics and biocidal activity. Materials Science and Engineering C, 2012, 32, 2381-2389.	3.8	51
111	Synthesis and study of magnetic properties of NiFe2O4 nanoparticles by PVA assisted auto-combustion method. Journal of Materials Science: Materials in Electronics, 2012, 23, 1011-1015.	1.1	13
112	A simple wet chemical route to synthesize ferromagnetic nickel ferrite nanoparticles in the presence of oleic acid as a surfactant. Journal of Materials Science: Materials in Electronics, 2012, 23, 1041-1044.	1.1	6
113	Effects of multiple organic ligands on size uniformity and optical properties of ZnSe quantum dots. Materials Research Bulletin, 2012, 47, 1892-1897.	2.7	16
114	Synthesis of wurtzite ZnS nanorods by microwave assisted chemical route. Materials Letters, 2012, 66, 276-279.	1.3	22
115	Preparation and properties of NiFe2O4 nanowires. Materials Letters, 2012, 66, 314-317.	1.3	39
116	Synthesis of highly size confined ZnS quantum dots and its functional characteristics. Materials Letters, 2012, 68, 78-81.	1.3	18
117	Synthesis of Fe3O4 nanoflowers by one pot surfactant assisted hydrothermal method and its properties. Materials Letters, 2012, 70, 73-75.	1.3	30
118	Organic ligand assisted low temperature synthesis of lead sulfide nanocubes and its optical properties. Materials Letters, 2012, 71, 44-47.	1.3	7
119	Growth and characterization of novel organic optical crystal: Anilinium d-tartrate (ADT). Spectrochimica Acta - Part A: Molecular and Biomolecular Spectroscopy, 2012, 87, 265-272.	2.0	20
120	Uniaxial growth of ã€^100〉 zinc (tris) thiourea sulphate (ZTS) single crystal by Sankaranarayanan–Ramasamy (SR) method and its characterizations. Spectrochimica Acta - Part A: Molecular and Biomolecular Spectroscopy, 2012, 94, 265-270.	2.0	7
121	Chemical synthesis of monodispersed ZnSe nanowires and its functional properties. Materials Letters, 2012, 81, 59-61.	1.3	16
122	Monodispersed synthesis of hierarchical wurtzite ZnS nanostructures and its functional properties. Materials Letters, 2012, 81, 209-211.	1.3	10
123	Synthesis of TiO2 nanoparticles with mesoporous spherical morphology by a wet chemical method. Materials Letters, 2012, 82, 208-210.	1.3	15
124	Zinc oxide nanoparticles: A study of defect level blue–green emission. Optical Materials, 2012, 34, 817-820.	1.7	25
125	Synthesis and characterization of NiO nanoparticles by sol–gel method. Journal of Materials Science: Materials in Electronics, 2012, 23, 728-732.	1.1	162
126	Influence of lanthanide ion on the morphology and luminescence properties of cadmium sulphide nanocrystals. Journal of Alloys and Compounds, 2011, 509, 5816-5821.	2.8	7

#	Article	IF	CITATIONS
127	Structural and magnetic properties of iron, cobalt and nickel nanoparticles. Synthetic Metals, 2011, 161, 1776-1780.	2.1	24
128	Effect of urea and thiourea on nonlinear optical hippuric acid crystals. Journal of Physics and Chemistry of Solids, 2011, 72, 1273-1278.	1.9	14
129	Synthesis and characterization of nickel ferrite magnetic nanoparticles. Materials Research Bulletin, 2011, 46, 2208-2211.	2.7	137
130	Preparation and properties of nickel ferrite (NiFe2O4) nanoparticles via sol–gel auto-combustion method. Materials Research Bulletin, 2011, 46, 2204-2207.	2.7	178
131	Observation of magnetic, structural and surface morphological studies of triangle-like nickel nanoplates. Materials Letters, 2011, 65, 310-313.	1.3	2
132	Synthesis and characterization of NiFe2O4 nanosheet via polymer assisted co-precipitation method. Materials Letters, 2011, 65, 483-485.	1.3	104
133	Preparation of sheet like polycrystalline NiFe2O4 nanostructure with PVA matrices and their properties. Materials Letters, 2011, 65, 1438-1440.	1.3	74
134	Solvothermal synthesis of nickel nanorods and its magnetic, structural and surface morphological behavior. Materials Letters, 2011, 65, 1565-1568.	1.3	10
135	Synthesis and vibrational properties of hematite (α-Fe2O3) nanoparticles. Journal of Materials Science: Materials in Electronics, 2011, 22, 1357-1360.	1.1	10
136	Preparation and characterization of NiFe2O4 nanoparticles. Transactions of the Indian Institute of Metals, 2011, 64, 233-234.	0.7	2
137	Organic molecules passivated Mn doped Zinc Selenide quantum dots and its properties. Applied Surface Science, 2011, 257, 7699-7703.	3.1	9
138	Crystal growth, structure and characterizations of a new semiorganic nonlinear optical material $\hat{a} \in \hat{a}^{2}$ -Alanine zinc chloride. Materials Research Bulletin, 2010, 45, 897-904.	2.7	29
139	Synthesis of organic ligand passivated zinc selenide nanorods via wet chemical route. Materials Letters, 2010, 64, 2094-2097.	1.3	14
140	Effect of strontium chloride on the optical and mechanical properties of γ–glycine crystals. Crystal Research and Technology, 2010, 45, 497-502.	0.6	27
141	Synthesis and properties of αâ€Fe <sub>2</sub> O <sub>3</sub> nanorods. Crystal Research and Technology, 2010, 45, 965-968.	0.6	55
142	Growth, optical, thermal, piezo and ferroelectric studies on ethylenediamine ditartrate dihydrate (EDADTDH) single crystals. Journal of Crystal Growth, 2010, 312, 1040-1045.	0.7	15
143	Growth and characterization of a solution grown, new organic crystal: l-histidine-4-nitrophenolate 4-nitrophenol (LHPP). Journal of Crystal Growth, 2010, 313, 30-36.	0.7	39
144	Crystal growth and characterizations of l-cystine dihydrobromide—A semiorganic nonlinear optical material. Physica B: Condensed Matter, 2010, 405, 1119-1124.	1.3	13

#	Article	IF	CITATIONS
145	Temperature dependence of morphology, structural and optical properties of ZnS nanostructures synthesized by wet chemical route. Journal of Alloys and Compounds, 2010, 506, 249-252.	2.8	22
146	Optical and surface morphological properties of triethylamine passivated lead sulphide nanoparticles. Materials Chemistry and Physics, 2009, 117, 443-447.	2.0	32
147	Optical, structural and surface morphological studies of bean-like triethylamine capped zinc selenide nanostructures. Materials Letters, 2009, 63, 1931-1934.	1.3	20
148	Inorganic surface passivation of CdS nanocrystals resulting in strong luminescence. Journal of Alloys and Compounds, 2009, 486, 844-847.	2.8	7